EVALUATION OF INTERFERENCE-CANCELLATION BASED MAC PROTOCOLS FOR VEHICULAR COMMUNICATIONS

A Thesis

by

KIRAN KUMAR GOGINENI VISHNU

Submitted to the Office of Graduate and Professional Studies of
Texas A&M University
in partial fulfillment of the requirements for the degree of

MASTER OF SCIENCE

Chair of Committee,	Krishna R. Narayanan
Co-Chair of Committee,	Scott L. Miller
Committee Members,	Jose Silva-Martinez
	Anxiao (Andrew) Jiang
Head of Department,	Miroslav M. Begovic

August 2017

Major Subject: Electrical Engineering

ABSTRACT

Vehicular communications form an important part of future intelligent transport systems. Wireless connectivity between vehicles can enhance safety in vehicular networks and enable new services such as adaptive traffic control, collision detection and avoidance. As several new algorithms are being developed for enhancing vehicle to vehicle wireless connectivity, it is important to validate the performance of these algorithms using reasonably accurate wireless channel models. Specifically, some recent developments in the medium access control (MAC) layer algorithms appear to have the potential to improve the performance of vehicle to vehicle communications; however, these algorithms have not been validated with realistic channel models encountered in vehicular communications.

The aforementioned issues are addressed in this thesis and correspondingly, there are two main contributions - (i) A complete IEEE 802.11p based transceiver model has been simulated in MATLAB and its performance & reliability are tested using existing empirically-developed wireless channel models. (ii) A new MAC layer algorithm based on slotted ALOHA with successive interference cancellation(SIC) has been evaluated and tested by taking into consideration the performance of underlying physical layer. The performance of slotted ALOHA-SIC and the already existing carrier sense multiple access with collision avoidance (CSMA/CA) scheme with respect to channel access delay and average packet loss ratio is also studied.

DEDICATION

To my mother Anuradha, my sister Laxmi and my father Madhusudhan and to my close friends Vamshi, Santhosh and Shashank.

ACKNOWLEDGMENTS

First and most importantly, I would like to thank my advisor, Dr. Krishna R. Narayanan for helping me complete this thesis. Working with Dr. Narayanan has enriched my academic knowledge and his achievements and works ethics have been an inspiration to me.

I would also like to thank my Graduate Committee Members Dr. Scott L. Miller, Dr. Anxiao Jiang and Dr. Jose Silva-Martinez for spending their valuable time with my thesis.

I also want to thank my colleagues and friends Digveer, Abhishek, Nagaraj, Dinesh, Surya and Hussain for making this period enjoyable.

CONTRIBUTORS AND FUNDING SOURCES

Contributors

This work was supported by Professor Krishna R. Narayanan [advisor] of the ECE Department at Texas A&M University.

All other work conducted for the thesis was completed by the student independently.

Funding Sources

Graduate study was partly supported by a student assistant position from ECE Department at Texas A&M University.

NOMENCLATURE

AIFS	Arbitration Inter-Frame Space
APDP	Average Power Delay Profile
AWGN	Additive White Gaussian Noise
BPSK	Binary Phase Shift Keying
CDF	Cumulative Distribution Function
CRC	Cyclic Redundancy Check
EDCA	Enhanced Distribution Channel Access
FCS	Frame Check Sequence
CRDSA	Contention Resolution Diversity Slotted ALOHA
CSMA/CA	Carrier Sense Multiple Access with Collision Avoidance
FDMA	Frequency Division Multiple Access
FEC	Forward Error Correction
GPS	Global Positioning System
IRSA	Irregular Repetition slotted ALOHA
LS	Least Squares
LLC	Logical Link Control
MAC	Medium Access Control Layer
MMSE	Minimum Mean Square Error
MPDU	MAC Protocol Data Unit
MSDU	MAC Service Data Unit

OFDM	Orthogonal Frequency Division Multiplexing
PAPR	Peak to Average Power Ratio
PCLP	Physical Layer Convergence Protocol
PHY	Physical Layer
PEC	Packet Erasure Channel
PLR	Packet Loss Ratio
PMD	Physical Medium Dependent
PPDU	Physical Layer Protocol Data Unit
PSDU	Physical Layer Protocol Data Unit
QAM	Quadrature Amplitude Modulation
QOS	Quality Of Support
QPSK	Quadrature Phase Shift Keying
RSSI	Received Signal Strength Indicator
RTV	Road To Vehicle
SIC	Successive Interference Cancellation
SNR	Signal to Noise Ratio
SIFS	Short Inter-Frame Space
TDL	Tap Delay Line
TDMA	Time Division Multiple Access
VANET	Vehicular Ad-Hoc Networks
V2I	Vehicle-to-Infrastructure
V2V	Vehicle-to-Vehicle
WAVE	Wireless Access in Vehicular Environments
WLAN	Wireless Local Area Network

TABLE OF CONTENTS

Page

LIST OF FIGURES

FIGURE Page

LIST OF TABLES

TABLE Page

1. INTRODUCTION

Wireless vehicle-to-vehicle(V2V) and vehicle-to-infrastructure(V2I) communications providing robust connectivity at moderate data rates have emerged as interesting research topics in recent years due to their impact on making transportation safer, autonomous and efficient. Development of vehicular ad hoc networks (VANET's) require accurate models for estimating the propagation channel and for determining the achievable packet transmission delay and reliability at the physical layer.

Based on the IEEE 802.11 wireless LAN standard [2], a standard termed as IEEE 802.11p was proposed [3] for implementing VANET's to provide wireless access in vehicular environments (WAVE). Together, these standards provide the specifications for the wireless LAN medium access control (MAC) and physical layers (PHY).

1.1 Physical Layer

Aimed at transmission over 5.725-5.825 GHz band with 10 MHz channel spacings , the PHY entity specifies an orthogonal frequency division multiplexing (OFDM) system with data payload communication capabilities of 3, 4.5, 6, 9, 12, 18, 24, and 27 Mb/s. The system uses 52 subcarriers that are modulated using binary or quadrature phase shift keying (BPSK or QPSK) or using 16- or 64-quadrature amplitude modulation (16-QAM or 64-QAM). Forward error correction coding (convolutional coding) is used with a coding rate of 1/2, 2/3, or 3/4 [4].

Since the V2V propagation channel has a significant impact on the performance of communication system in VANET's, extensive research efforts have been

made and two types of empirical vehicular channel models have been proposed [5]. The first one is a small scale fading model based on Tap-Delay Line(TDL) model [6] with Rayleigh/Rician fading on each tap while the second one is a large scale model with Nakagami-m fading where m represents the fading intensity and average recieved power [7]. These channel models successfully model fading & path-loss of V2V channels and provide reasonably accurate estimates of packet reception probability and loss ratio.

1.2 MAC Layer

Examining the 802.11p standard from the MAC layer perspective, carrier sense multiple access with collision avoidance(CSMA/CA) contention scheme, which has been already in use in the Wi-Fi standard [2] has been proposed for V2V scenarios also. However, in an ad-hoc highway scenario with periodic broadcast of time-critical packets, it has been shown that CSMA results in a drop of large number of packets because of the large delay associated with accessing the channel [1, 8].

In order to overcome this problem, many solutions have been proposed based on either Time Division Multiple Access(TDMA) [1] or slotted ALOHA [9]. These schemes divide a fixed frequency channel into different time slots so that the contending users in a system transmit in their own time slots assuming that the users are network synchronized. These schemes however require a learning phase, increasing the channel access delay and they cannot guarantee high reliability as the transmission error during learning phase renders the protocol to be unusable. Most importantly, transmission by two or more users in the same time slot results in collisions which are discarded and that time slot is essentially rendered useless.

Recently, an improved version of classical slotted ALOHA was proposed for

satellite access packet networks which combines diversity transmission of data bursts with efficient interference cancellation techniques [10, 11]. Each packet was transmitted twice by an user in a random fashion followed by successive interference cancellation(SIC) at receiver resulting in a better delay and throughput performance. An improved version of this protocol is also proposed where an user transmits multiple copies instead of two based on a degree distribution [12, 13] with an application of adapting it to vehicular environments [8].

However, most of these research entities focus entirely on MAC layer and use idealized physical layer models. They do not take into account the effect of propagation environment on the performance of lowest layer (i.e. the physical layer), and therefore on the performance of entire system. In this thesis, we provide a joint PHY-MAC simulation [2] and study the performance of slotted ALOHA with SIC [8] and compare the results with the already existing CSMA/CA implementation taking into consideration all of the above mentioned details.

1.3 Contributions of this Thesis

The main contributions of this thesis can be summarized as follows:

- Implementation of IEEE 802.11p physical layer for vehicular communications as per the standard [2, 3].
- Implementation of a wireless fading channel encountered in vehicular environments [6, 7] for calculating average packet loss ratio and reliability analysis of the transmission.
- Implementation of slotted-ALOHA based MAC layer algorithm with successive interference cancellation(SIC) for scheduling channel availability in multi-user vehicular environment [12, 8] and optimization of parameters.

- Performance comparison between slotted-ALOHA with SIC and CSMA/CA in vehicular networks under a joint PHY-MAC Layer simulation with respect to reliability and delay incurred for successful transmission.

2. PHYSICAL LAYER OF IEEE 802.11P STANDARD

2.1 Introduction

The physical (PHY) & medium access control (MAC) layers for the vehicular communications have been implemented based on the IEEE 802.11-2012 [2] standard with further modifications to the standard proposed continuously. IEEE 802.11 standards offer several physical layer descriptions and one common MAC sub-layer with quality of service (QoS) support. IEEE 802.11p uses the orthogonal frequency division multiplexing (OFDM) physical layer detailed in clause 17 of 802.11 [2]. MAC Layer uses the carrier sense multiple access protocol detailed in clause 10 of 802.11 [2]. The following sections give a description of OFDM PHY layer implemented in this thesis.

PHY Layer further consists of a Physical Medium Dependent (PMD) sublayer and Physical Layer Convergence Protocol (PLCP) sublayer (shown in Table 2.1). The PMD sublayer defines the signal build up parameters, such as channel coding, modulation and the conversion of signal into analog form with reference to specific PHY type. PLCP ensures that the MAC layer receive packets of same format, independent of particular PMD sublayer by dealing with the differences among various PHY's.

OSI Layer	**Sub-Layers**
Data Link Layer	Logical Link Control (LLC)
	Medium Access Control (MAC)
Physical Layer	Physical Layer Convergence Protocol (PCLP)
	Physical Medium Dependent (PMD)

Table 2.1: Sub-layers of PHY & Link layers

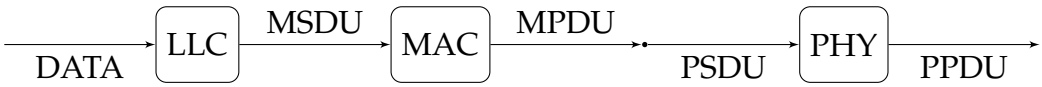

Figure 2.1: Relations among the MAC & physical layer's service data unit and protocol data unit.

The following notations are used in 802.11 for the PHY & MAC layer descriptions. The data payload received from upper layers is attached to headers and trailers at both the MAC and PHY before it gets transmitted. For example, each MAC Service Data Unit (MSDU) received from the Logic Link Control (LLC) layer is appended with a 30-byte-long MAC header and a 4-byte-long Frame Check Sequence (FCS) trailer to form the MAC Protocol Data Unit (MPDU). The same MPDU, once handed over to the PHY, is then called the Physical Layer Service Data Unit (PSDU). And, then a Physical Layer Convergence Procedure (PLCP) preamble and header, and proper tail bits and pad bits are attached to the PSDU to finally generate the Physical Layer Protocol Data Unit (PPDU) for transmission. The relationships among MSDU, MPDU, PSDU, and PPDU are illustrated in the Figure 2.1.

2.2 MAC Layer

MAC Header (30 octets)							**DATA** (variable octets)	**CRC-32** (4 octets)
2	2	6	6	6	2	6	0-2312	4
Frame Control	Durati -on/ID	Addr -ess 1	Addr -ess 2	Addr -ess 3	Sequence Control	Addr -ess 4	Frame Body	FCS

Table 2.2: MAC frame format

The MAC frame format for 802.11 is given in Table 2.2. Data received from the logical link control (LLC) layer is added with a MAC header 30 bytes of size. The MAC header contains information regarding the to and from addresses, power and sequence control. MAC header is followed by the frame data which can be variable in size ranging from 0 to 2312 bytes. A CRC-32 frame check sequence (FCS) of 4 bytes is added to the tail for error detection.

2.3 Physical Layer

A complete block diagram of the OFDM based transceiver is shown in Figure 2.2. Aimed at transmission over 5.725-5.825 GHz band with 10 MHz channel spacings, the PHY entity of 802.11p specifies an OFDM system with data payload communication capabilities of 3, 4.5, 6, 9, 12, 18, 24, and 27 Mb/s [4]. Since, 802.11p is almost similar to 802.11a Wi-Fi standard, except for the channel bandwidth, a basic comparison between both of them is provided in the Tables 2.3 and 2.4.

Data sent to the PHY layer from MAC layer is processed through a series of signal processing blocks, transmitted and then decoded at the receiver. The following sections provide a brief description about each of the individual blocks used in the PHY layer. A schematic block diagram is shown in Figure 2.2.

2.4 Transmitter

2.4.1 Scrambler

A length-127 scrambler using the generator polynomial $S(x) = x^7 + x^4 + 1$ with an initial state of 1011101 is used to scramble transmit data and to descramble receive data. This avoids long sequences of zeros or ones in the transmitted sequence and eliminates the dependence of a signal's power spectrum upon the actual transmitted data, making it more dispersed to meet PAPR requirements.

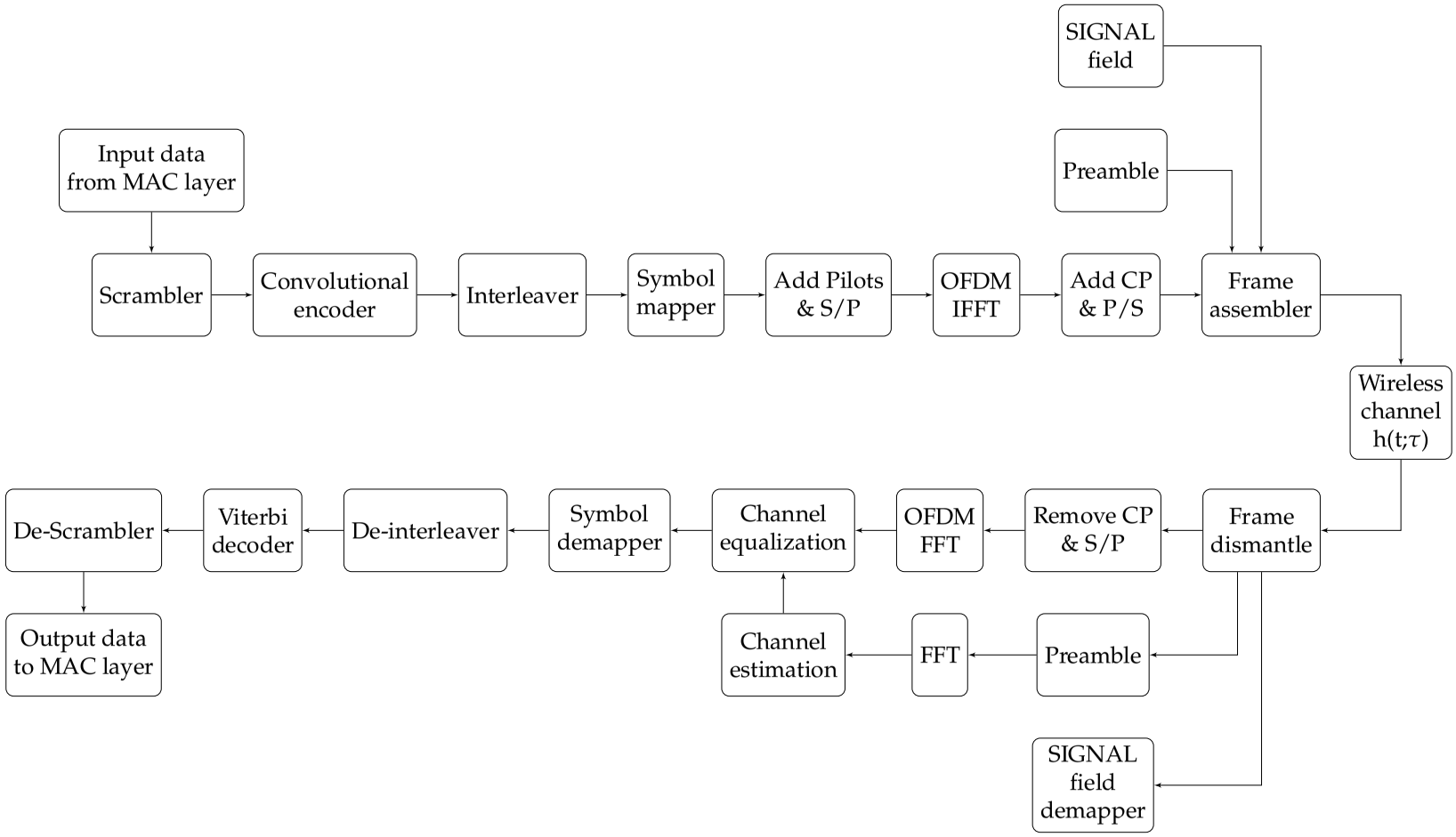

Figure 2.2: IEEE 802.11p PHY layer block diagram.

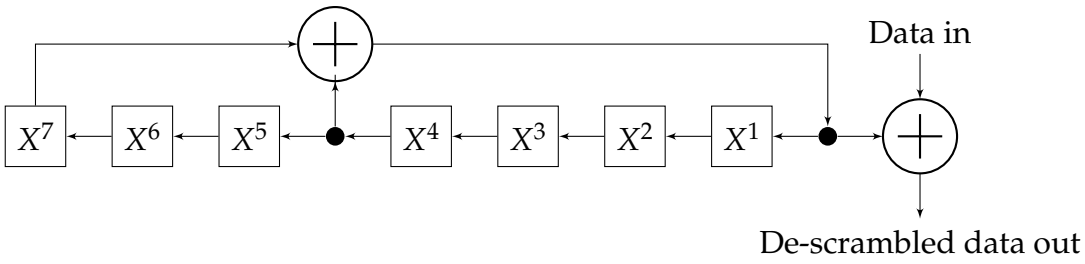

Figure 2.3: Scrambler

The scrambler implemented on 7 delay elements and 2 modulo-2 adders is shown in Figure 2.3.

2.4.2 Convolutional Encoder

For forward error correction, 802.11p uses a convolutional encoder of constraint length 7 with coding rates of $1/2$, $2/3$ or $3/4$, depending on the required transmission data rate. The generator polynomials used are $g_0 = 133_8$ and $g_1 = 171_8$ (subscript 8 refers to octal notation) of rate $1/2$ as shown in Figure 2.4 below. Higher rates are obtained by puncturing the code. Decoding scheme based on the Viterbi algorithm is used at the receiver.

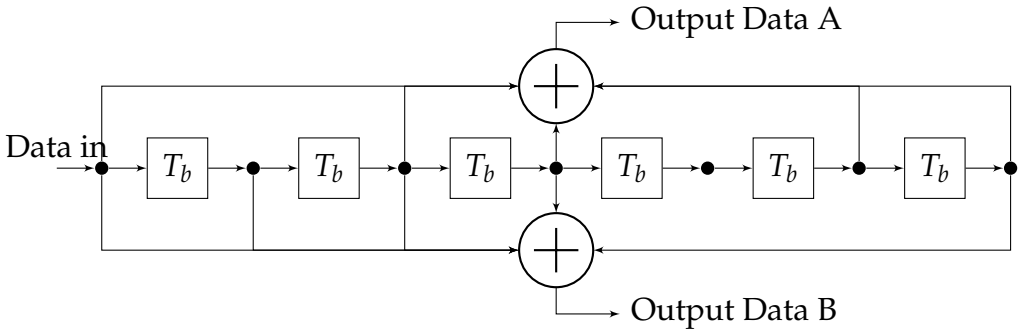

Figure 2.4: Convolutional Encoder

Parameter	*802.11p* Value (10 MHz channel spacing)	*802.11a* Value (20 MHz channel spacing)
N_{SD}: Number of data subcarriers	48	48
N_{SP}: Number of pilot subcarriers	4	4
N_{ST}: Number of subcarriers, total	$52(N_{SD} + N_{SP})$	$52(N_{SD} + N_{SP})$
Δ_F: Subcarrier frequency spacing	$0.15625MHz$ $(= 10MHz/64)$	$0.3125MHz$ $(= 20MHz/64)$
T_{FFT}: Inverse Fast Fourier Transform (IFFT) / Fast Fourier Transform (FFT) period	$6.4\mu s$ $(1/\Delta_F)$	$3.2\mu s$ $(1/\Delta_F)$
$T_{PREAMBLE}$: PLCP preamble duration	$32\mu s$ $(T_{SHORT} + T_{LONG})$	$16\mu s$ $(T_{SHORT} + T_{LONG})$
T_{SIGNAL}: Duration of the SIGNAL BPSK-OFDM symbol	$8.0\mu s$ $(T_{GI} + T_{FFT})$	$4.0\mu s$ $(T_{GI} + T_{FFT})$
T_{GI}: GI duration	$1.6\mu s$ $(T_{FFT}/4)$	$0.8\mu s$ $(T_{FFT}/4)$
T_{GI2}: Training symbol GI duration	$3.2\mu s$ $(T_{FFT}/2)$	$1.6\mu s$ $(T_{FFT}/2)$
T_{SYM}: Symbol interval	$8\mu s$ $(T_{GI} + T_{FFT})$	$4\mu s$ $(T_{GI} + T_{FFT})$
T_{SHORT}: Short training sequence duration	$16\mu s$ $(10 \times T_{FFT}/4)$	$8\mu s$ $(10 \times T_{FFT}/4)$
T_{LONG}: Long training sequence duration	$16\mu s$ $(T_{GI2} + 2 \times T_{FFT})$	$8\mu s$ $(T_{GI2} + 2 \times T_{FFT})$

Table 2.3: Timing-related parameters

2.4.3 Interleaver

For the purpose of reducing the burst errors caused by channel fading, the output data from the encoder is interleaved. A block interleaver is used in 802.11p for interleaving all the encoded data bits with the block size of interleaving equal to the number of bits in one OFDM symbol (N_{CBPS}). The interleaver uses a two step permutation process. The first step ensures that adjacent coded bits are mapped onto non-adjacent sub-carriers while the second step ensures that adjacent coded bits are mapped alternately onto both less and more significant bits of the constel-

lation thereby avoiding long runs of low-reliability bits.

					802.11p	*802.11a*
Modulation	**Coding rate (R)**	**Coded bits per subcarrier (N_{BPSC})**	**Coded bits per OFDM symbol (N_{CBPS})**	**Data bits per OFDM symbol (N_{DBPS})**	**Data rate (Mb/s) (10 MHz channel spacing)**	**Data rate (Mb/s) (20 MHz channel spacing)**
BPSK	1/2	1	48	24	3	6
BPSK	3/4	1	48	36	4.5	9
QPSK	1/2	2	96	48	6	12
QPSK	3/4	2	96	72	9	18
16-QAM	1/2	4	192	96	12	24
16-QAM	3/4	4	192	144	18	36
64-QAM	2/3	6	288	192	24	48
64-QAM	3/4	6	288	216	27	54

Table 2.4: Modulation-dependent parameters

2.4.4 Modulation

802.11p uses CP-OFDM with 64 sub-carriers as its modulation format, enabling high data rates. Only 52 of 64 sub-carriers are actually used for modulation and transmission while the other 12 subcarriers are null-carriers without any useful information. The 52 data sub-carriers are indexed from -26 to 26 along with a zero DC sub-carrier indexed at 0. 4 sub-carriers (-21, -7, 7, 21) are used as pilots for transmitting BPSK-modulated pseudo random sequence already known at the receiver. The remaining 48 sub-carriers are used to carry the PSDU data. Gray-coded BPSK, QPSK, 16-QAM or 64-QAM are used as the modulation formats, depending on the channel state.

An OFDM symbol uses a duration of $8\mu s(T_{FFT} + T_{GI})$, with a cyclic prefix duration of $1.6\mu s(T_{GI} = T_{FFT}/4)$. This guard interval duration has been proved to

be greater than the average delay spreads in typical vehicular channels in multiple field tests, thereby making the inter symbol interference (ISI) negligible [14].

Table 2.4 provides a summary of the rates that can be achieved with different combinations of coding rates and modulation schemes.

2.4.5 Training Sequences

Training sequences comprising 10 short symbols & 2 long symbols are used in the PCLP preamble field for synchronization and channel estimation purposes.

The preamble field starts out with 10 short symbols of duration $1.6\mu s$ each that allows for the receiver to detect the signal and perform frequency offset correction. The short symbols consist of 12 sub-carriers, modulated by elements of following sequence:

$S_{-26,26} = \sqrt{(13/6)}\{0,0,1+j,0,0,0,-1-j,0,0,0,1+j,0,0,0,-1-j,0,0,0,$
$-1-j,0,0,0,1+j,0,0,0,0,0,0,0,-1-j,0,0,0,-1-j,0,0,0,1+j,0,0,0,1+j,$
$0,0,0,1+j,0,0,0,1+j,0,0\}$.

The short symbols are followed by 2 long training symbols each of $8\mu s$ duration that are used for both channel estimation and finer frequency offset estimation. Each long training symbol consists of 53 sub-carriers, modulated by elements of sequence L given by:

$L_{-26,26} = \{1,1,-1,-1,1,1,-1,1,-1,1,1,1,1,1,1,-1,-1,1,1,-1,1,-1,1,1,$
$1,1,0,1,-1,-1,1,1,-1,1,-1,1,-1,-1,-1,-1,-1,1,1,-1,-1,1,-1,1,-1,1,$
$1,1,1\}$.

2.4.6 PPDU Packet Formation

Table 2.5 explains the arrangement of a PPDU packet to be transmitted after PMD sub-layer. The preamble consisting of 2 long and 10 short training sequences followed by a SIGNAL field containing information regarding data transmission

PHY PMD Layer	PCLP Preamble (4 OFDM symbols(2+2))		SIGNAL (1 OFDM symbol)	DATA (variable OFDM symbols)
	Short training (10 symbols)	Long training (2 symbols)	Coded/OFDM BPSK,r=1/2	Coded/OFDM, TX rate indicted in SIGNAL

Table 2.5: PHY protocol data unit (PPDU) frame format

rate are added as headers to the data part forming a PPDU packet.

2.5 Receiver

The receiver block is designed to invert the channel operation and extract the necessary packet information. Assuming ideal frequency and phase offset correction at the receiver, following steps are performed at the receiver:

1. The preamble and signal field of the received PPDU frame are separated from the data part.

2. Information regarding data transmission rate and the modulation scheme used are extracted from the signal field.

3. Cyclic prefix is removed from the preamble and data and an FFT operation $(N_{FFT} = 64)$ is performed to convert them into frequency domain.

4. The 2 long symbols of the preamble part are used to estimate the channel state information.

5. Using a one-tap frequency domain equalizer (FEQ) , the channel impulse response is inverted.

6. Each sub-carrier is then demodulated by its respective symbol mapping scheme and then de-interleaved.

7. The data is then decoded using a soft decision Viterbi decoder to decode the convolutionally encoded information and restored to its original state using the descrambler.

The channel estimation and equalization blocks are explained in detail below.

2.5.1 Frequency-Domain Channel Estimation

OFDM systems are potentially able to mitigate ISI introduced by the channel as long as the cyclic prefix is greater than the channel impulse response. Also, since the cyclically extended guard interval turns the linear convolution of channel into circular convolution, the frequency-selective fading channel can be converted into a number of flat fading channels.

Assuming that an input OFDM data stream $x[n]$ is sent through a channel with impulse response $h[n]$, the input at receiver $y[n]$ can be assumed as:

$$y[n] = h[n] \circledast x[n] + w[n],$$

where $\circledast$ signifies circular convolution and $w[n]$ is the noise added to the transmitted signal.

Consequently, the discrete frequency transmission equation after the cyclic prefix removal and FFT operation can be summarized as:

$$Y_i(k) = H_i(k)X_i(k) + W_i(k),$$

where k denotes the k-th sub-carrier of the i-th OFDM symbol.

802.11p uses data aided channel estimation technique with the help of two long symbols in the preamble. The most straightforward principle is to extract coefficients from the two long symbols already known at the receiver using the

least squares estimate(LS). The channel coefficient of the k-th sub-carrier using the LS estimate can be calculated with

$$H_p^{LS}(k) = \frac{Y_p(k)}{X_p(k)}$$

where p denotes preamble sequence. Since two long training symbols are present, the final channel estimate is given by the average of two estimates obtained independently from each symbol as

$$H_p^{LS}(k) = \frac{H_{p1}^{LS}(k) + H_{p2}^{LS}(k)}{2}$$

Comparing the LS estimate with the original transmission equation, we have

$$H_p^{LS}(k) = H_p(k) + \frac{W_p(k)}{X_p(k)}$$

This shows that the LS estimation is simple but not very robust in high interference or noise environments. This can be improved by averaging the LS estimates over a number of symbols, or by MMSE estimation which further minimizes the minimum mean square error. The LMMSE channel estimate can be computed as:

$$H_p^{LMMSE}(k) = R_H(R_H + \sigma^2(X_p X_p^H)^{-1})^{-1} H_p^{LS}(k)$$

MMSE estimation is usually more reliable, since it forms a more conservative channel estimate based on strength of noise variance (σ^2) and statistics of the channel covariance matrix R_H. However, the channel covariance matrix $R_H = E[HH^H]$ needs to be known a priori at the receiver which is not generally possible and the matrix inversion further increases the computational complexity.

Further improvements to estimation can be obtained via decision feedback techniques where the data outputs from the Viterbi decoder are used to estimate the channel using a feedback loop at the receiver [15]. Also, pilots at the four sub-carriers (-21,-7,7,21) can be used for further improvement via interpolation techniques [16].

2.5.2 Frequency Equalization

Equalizer is generally used to reduce or eliminate ISI by simply reversing the distortions introduced by the channel. For CP-OFDM, assuming that channel state information is calculated using one of the above mentioned estimation techniques, a simple frequency domain equalization can be performed using a one-tap equalizer (zero-forcing equalizer) by inverting the channel response as follows:

$$\hat{X}(k) = \frac{Y(k)}{H(k)},$$

where k denotes the k-th sub-carrier. This results in :

$$\hat{X}(k) = X(k) + \frac{W(k)}{H(k)}.$$

The noise component enhancement from zero-forcing strategy can be mitigated by using a frequency domain MMSE equalizer given by:

$$\hat{X}(k) = \frac{Y(k)H^H(k)}{(H^H(k)H(k) + \sigma^2)}.$$

This is equivalent to ZF equalizer except for the noise term, so in the absence of noise both the equalizers are equivalent.

2.6 Our Implementation

We have developed a MATLAB based PHY layer simulator based on the 802.11p standard [2]. The following blocks were implemented:

- At the transmitter section, scrambler, convolutional encoder, interleaver and symbol mapper with provision for the 8 types of data rates are modeled.
- An OFDM modulator with cyclic prefix and a preamble section with long and short training sequences and SIGNAL field are modeled.
- On the receiver side, OFDM demodulator, symbol de-mapper, de-interleaver, soft-decision Viterbi decoder, de-scrambler are modeled.
- Channel estimation based on long training sequences with least square estimate and zero forcing equalizer are used for reference.
- Short training sequences are modeled but not used and time-domain windowing of OFDM sequences are not implemented in the current model.
- Bit error rate performance of system model is verified with theoretical limit of channel coding scheme in the presence of an AWGN channel.

3. WIRELESS CHANNEL MODELS

3.1 Introduction

A wireless propagation channel refers to the medium linking both transmitter and receiver. Its properties determine the specific behavior of wireless systems and their performance limit. Signal transmission over vehicular channels involves propagation over multiple paths with each path having line of sight or non-line of sight connection between transmitter and receiver and the relative motion in between them. Furthermore the transmitted signal can be scattered, reflected or diffracted by multiple objects depending on the environment.

Because of the sophisticated nature of the radio channel parameters, an accurate channel characterization can only be possible with appropriate channel measurements. This chapter presents two empirical channel models proposed for vehicular networks and their implementation.

3.2 Channel Properties

Multipath propagation between transmitter and receiver results in a signal which can be assumed as summation of the contribution of each individual path at the receiver. As a result the signal experiences fading with multiple delay paths defining the impulse response of channel. The expected power at different delays is generally defined by the average power delay profile(APDP), from which the root mean square (rms) delay spread can be evaluated. The mobility of users in case of vehicular networks also results in Doppler spread of signal which should be taken into account.

The following metrics are generally used to characterize wireless channels:

1. *Signal fading*
2. *Delay spread*
3. *Doppler spread*
4. *Angular spread*
5. *Path loss*
6. *Shadowing*

All of the above listed properties influence the channel characteristics. Depending on different scenarios, these metrics generally vary and as a result, a wireless system optimized for one scenario may not work as well in a completely different scenario.

3.3 Vehicular Channel Models

For system performance evaluation by simulation, two types of radio channel models are proposed for use in 802.11p networks : Acosta-Marum & Ingram Model [6] and Cheng *et al.* Model [7].

3.3.1 Acosta-Marum & Ingram Model

The channel impulse response for a time-variant multipath channel is modeled with information at certain taps (delays). An empirical TDL model based on channel measurements is proposed for 802.11p by Acosta-Marum & Ingram is used as reference [6].

The channel model consists of a tapped delay line with uniformly spaced taps (Figure 3.1). For a signal transmitted through the channel with bandwidth W (10MHz for 802.11p), the tap spacing between adjacent taps is given by $1/W$ ($100ns$) which denotes the time resolution that can be achieved. The channel coefficients $c_i(t)$ denote either Rician or Rayleigh fading processes. The total length

of delay line denotes the time dispersion (multipath delay spread) of the channel.

Each of the tap coefficients are modeled as Rician-K/Rayleigh fading processes having their own respective Doppler spread and fading spectral shape. The required parameters are enumerated below:

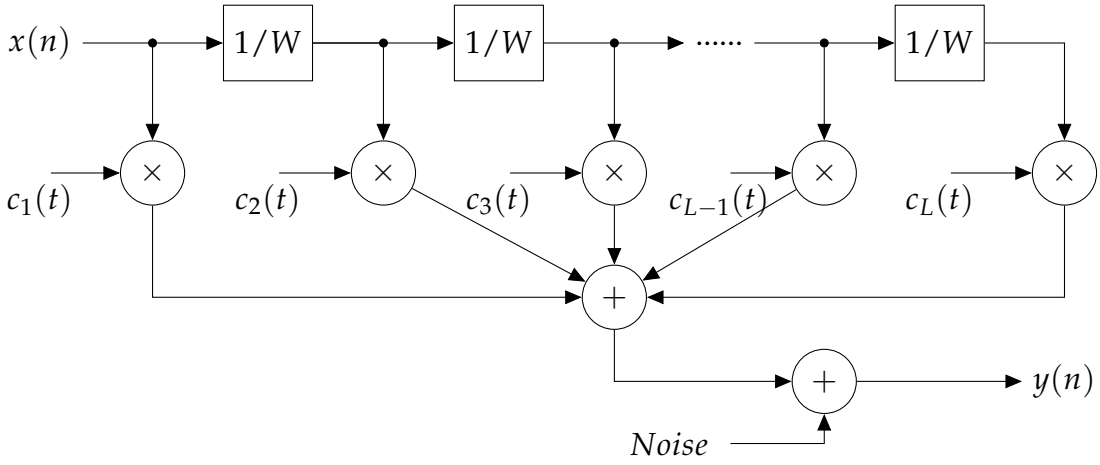

Figure 3.1: Tap-Delay Line Channel Model

1. Number of taps or paths
2. Relative time delay per tap
3. Relative path loss per tap
4. Amplitude statistics and modulation (Rayleigh/Rician) per tap
5. Doppler spectrum shape and parameters per tap

In [6], channel measurements were performed in six scenarios in urban, suburban and expressway environments with vehicle speeds varying between 32-140km/hr. These models represent multipath fading effects for small-scale fading only and do not include log-normal shadowing or path loss.

Scenario	Distance between Tx & Rx(m)	Cumulative Speed v (km/hr)	Max. Delay spread $\tau_s(\mu s)$
V2V - Expressway oncoming	300-400	210	0.3
V2V - Urban canyon oncoming	100	32-48	0.5
RTV - Suburban street	100	32-48	0.4
RTV - Expressway	300-400	105	0.4
V2V - Expressway same direction with wall	300-400	105	0.7
RTV - Urban canyon	100	32-48	0.7

R - Roadside, V - Vehicle

Table 3.1: Parameters of Six TDL Channel models

A brief summary of the six models with their respective measurement parameters are summarized in Table 3.1 and the fading parameters for one channel model (Vehicle to Vehicle Expressway Oncoming) are listed in Table 3.2 [6].

Tap No.	Path No.	Tap Power (dB)	Relative PathLoss (dB)	Delay Value (ns)	Rician K (dB)	Freq. Shift (Hz)	Fading Doppler (Hz)	LOS Doppler (Hz)	Modulation	Fad.Spec. Shape
1	1	0.0	0.0	0	-1.6	1451	60	1452	Rician	Round
1	2		-24.9	1	n/a	884	858	n/a	Rayleigh	Round
1	3		-25.5	2	n/a	1005	486	n/a	Rayleigh	Round
2	4	-6.3	-13.1	100	n/a	761	655	n/a	Rayleigh	Classic 3dB
2	5		-7.5	101	n/a	1445	56	n/a	Rayleigh	Round
3	6	-25.1	-28.9	200	n/a	819	823	n/a	Rayleigh	Classic 3dB
3	7		-28.9	200	n/a	819	823	n/a	Rayleigh	Classic 3dB
3	8		-35.6	202	n/a	124	99	n/a	Rayleigh	Round
4	9	-22.7	-25.7	300	n/a	1437	110	n/a	Rayleigh	Flat
4	10		-34.4	301	n/a	552	639	n/a	Rayleigh	Classic 3dB
4	12		-27.4	302	n/a	868	858	n/a	Rayleigh	Classic 6dB

Table 3.2: V2V Expressway Oncoming - TDL channel model

3.3.2 Cheng's Model

This channel impulse response model is based on the narrow-band measurements of mobile vehicle-to-vehicle propagation channel at 5.9 GHz, under realistic suburban driving conditions based on the study by Lin Cheng *et al.* [7].

Using two large data sets taken in suburban environments, single-slope and dual-slope large-scale path loss models including log-normal fading were proposed. An analysis of the observed fading statistics using Nakagami-m distribution was presented where the fading gradually transitions from near Rician to Rayleigh as the separation between vehicles increases. It is also observed that at large distances, the fading can be more severe than Rayleigh.

Path Loss Models:

Using RSSI measurements and distance between vehicles, the path loss measurements can be presented via a single-slope log-normal model as

$$P_r(d) = P_r(d_0) + 10\gamma \log\left(\frac{d}{d_0}\right) + X_\sigma$$

where $P_r(d)$ and $P_r(d_0)$ are the received signal strengths at distance d and at reference distance d_0 respectively. The path-loss exponent(γ) and log-normal random variable (X_σ; X - zero-mean normally distributed random variable with standard deviation σ) for shadowing are estimated via linear regression on the datasets. The $P_r(d_0)$ (dBm) is calculated using the following free space path gain equation.

$$P_r(d_0)(dBm) = P_t(dBm) - 10\log\left(\frac{\lambda^2}{(4\pi)^2 d_0^2}\right)$$

where d_0 is reference distance of $10m$ and λ is wavelength for carrier frequency of $f = 5.9$ GHz.

Parameter	**Data Set 1**	**Data Set 2**
Single slope γ	2.75	2.32
Single slope $\sigma(dB)$	5.5	7.1
Dual slope γ_1	2.1	2
Dual slope $\sigma_1(dB)$	2.6	5.6
dual slope γ_2	3.8	4
Dual slope $\sigma_2(dB)$	4.4	8.4
Critical distance $d_c(m)$	100	100

Table 3.3: Large-scale path loss model parameters

Since in practice, a dual-slope piecewise-linear model represents more accurately the measurements, the same was characterized based on the formula below:

$$P_r(d) = \begin{cases} P_r(d_0) - 10\gamma_1 \log_{10}(\frac{d}{d_0}) + X_{\sigma_1} & \text{if } d_0 \leq d \leq d_c \\ P_r(d_0) - 10\gamma_1 \log_{10}(\frac{d_c}{d_0}) - 10\gamma_2 \log_{10}(\frac{d}{d_c}) + X_{\sigma_2} & \text{if } d_0 \leq d \leq d_c \end{cases}$$

where d_c represents the critical distance below which the path loss exponent (γ_1) and standard deviation (σ_1) hold good. Beyond the critical distance, signal strength falls off with another path loss exponent (γ_2) with a standard deviation (σ_2) . The piecewise linear fit of these models to the measurement datasets are presented in the Table 3.3.

Fading Analysis:

In [7], fading due to multipath was modeled based on Nakagami distribution since it is a more general model that can represent Rayleigh, Rician, or fading that is more severe than Rayleigh, depending on model parameters, and thus is capable of describing a wide range of fading situations given the varied nature of driving environments. The probability density function (PDF) for the Nakagami-

Dataset 1	
Distance bin(meters)	m
From 0.0 to 5.5	4.07
From 5.5 to 13.9	2.44
From 13.9 to 35.5	3.08
From 35.5 to 90.5	1.52
From 90.5 to 230.7	0.74
From 230.7 to 588.0	0.84

Dataset 2	
Distance bin(meters)	m
From 0.0 to 4.7	3.01
From 4.7 to 11.7	1.18
From 11.7 to 28.9	1.94
From 28.9 to 71.6	1.86
From 71.6 to 177.3	0.45
From 177.3 to 439.0	0.32

Table 3.4: Estimated values of shape parameter-m using channel measurements.

m distribution is given by:

$$f(x; m, P_r(d)) = \frac{2m^m x^{2m-1}}{[P_r(d)]^m \Gamma(m)} e^{\frac{mx^2}{P_r(d)}}$$

where m reprsents the fading intensity, $P_r(d)$ the average received power at a distance d, and $\Gamma(m)$ is the gamma function. When $m = 1$ the Nakagami distribution describes a Rayleigh distribution, while for $m > 1$ the distribution is Rician. channel conditions are worse than the Rayleigh distribution are obtained for $m < 1$. The values of m are distance dependent and are presented for the two datasets in the Table 3.4.

The fading analysis combined with the large scale path loss model can be used to generate random values of the received signal power at the selected distance between transmitter and receiver. This empirical model successfully takes into consideration the pathloss, fading and shadowing phenomenon based on the distance relationship. However, it does not address the effects of co-channel interference in the presence of large number of users which generally increases the noise floor, as the interference tends to Gaussian distribution through central limit theorem.

3.4 Our Implementation

Both of the channel models [6, 7] described above are modeled for usage with the PHY layer simulator.

- Based on [7], a large scale fading model with dual slope path loss and shadowing is implemented for the two datasets. Single-tap Nakagami-*m* fading is used for the small scale fading in this case.

- Based on [6, 17], small scale fading models based on six different environment scenarios are implemented. Each of these models use a tap delay line filter with each of the delay line co-efficients having Raleigh/Rician fading process and its own fading Doppler spectrum. These TDL fading models are used in the joint PHY-MAC simulations.

4. MAC LAYER - CONTENTION SCHEMES

4.1 Introduction

Since the frequency band assigned for communication purposes is generally a sparse resource, multiple access techniques are generally used to allow multiple users communicate over the same channel with maximum efficiency. Medium access control (MAC) protocol residing in the data link layer is responsible for regulating access to a shared medium. MAC protocols available in the literature are generally distinguished between centralized and distributed protocols and whether the channel access is guaranteed or random.

Random access protocols (e.g., ALOHA, CSMA etc.) make the individual users contend for channel access based on a set of criteria and as a result the channel access delay is not upper bounded or predictable whereas MAC protocols categorized as guaranteed (e.g., TDMA, FDMA etc.) allow for all users to transmit at a certain time frame and as a result, channel access is predictable and delay upper-bounded. Guaranteed channel access is generally easily obtained by a centralized network scheme with a central controller distributing the resources between contending users and in the case of distributed/ ad-hoc networks, random access schemes are more easy to implement.

In case of Vehicular ad-hoc networks (VANET's), the network is more distributed in nature. However, as most of the applications for VANET's include safety applications and time-critical messages, a MAC algorithm that is distributed, delay bounded and predictable in nature is generally more preferable.

802.11p standard defines the usage of CSMA/CA as the MAC layer contention scheme for usage in first generation VANET's. This chapter provides details of

CSMA scheme along with its limitations and the usage of slotted ALOHA based scheme with successive interference cancellation as an alternative.

4.2 Carrier Sense Multiple Access

IEEE 802.11p uses CSMA/CA with enhanced distribution channel access (EDCA) as its MAC contention scheme as described in IEEE 02.11-2012 standard. CSMA works by sensing the channel first, i.e., the user starts by listening to the channel, and if it is free for a certain amount of time period (called as arbitration inter-frame space (AIFS)), the user can start transmitting directly. If the channel is busy or becomes occupied during the AIFS, the user must perform a backoff, i.e., the user has to defer its access according to a randomized time period.Quality of service(QoS) is obtained based on the packet types, with low latency requirement packets having low AIFS values. Four priority queues are defined with higher priority queue having lower value of AIFS.

The back-off procedure in 802.11 is detailed below:

- selecting a number from the contention window (equivalent to drawing a number from uniform distribution[0, CW]; CW is the current contention window)
- setting up a back-off value which is equal to the product of random number drawn from CW and *slot time* derived from the PHY modulation parameters.
- decrementing the back-off only when the channel is free and upon reaching a back-off value of 0, send packet immediately.

A flowchart describing the back-off procedure and channel sensing is given in Figure 4.1 for the broadcast scenario [referred from [1]].

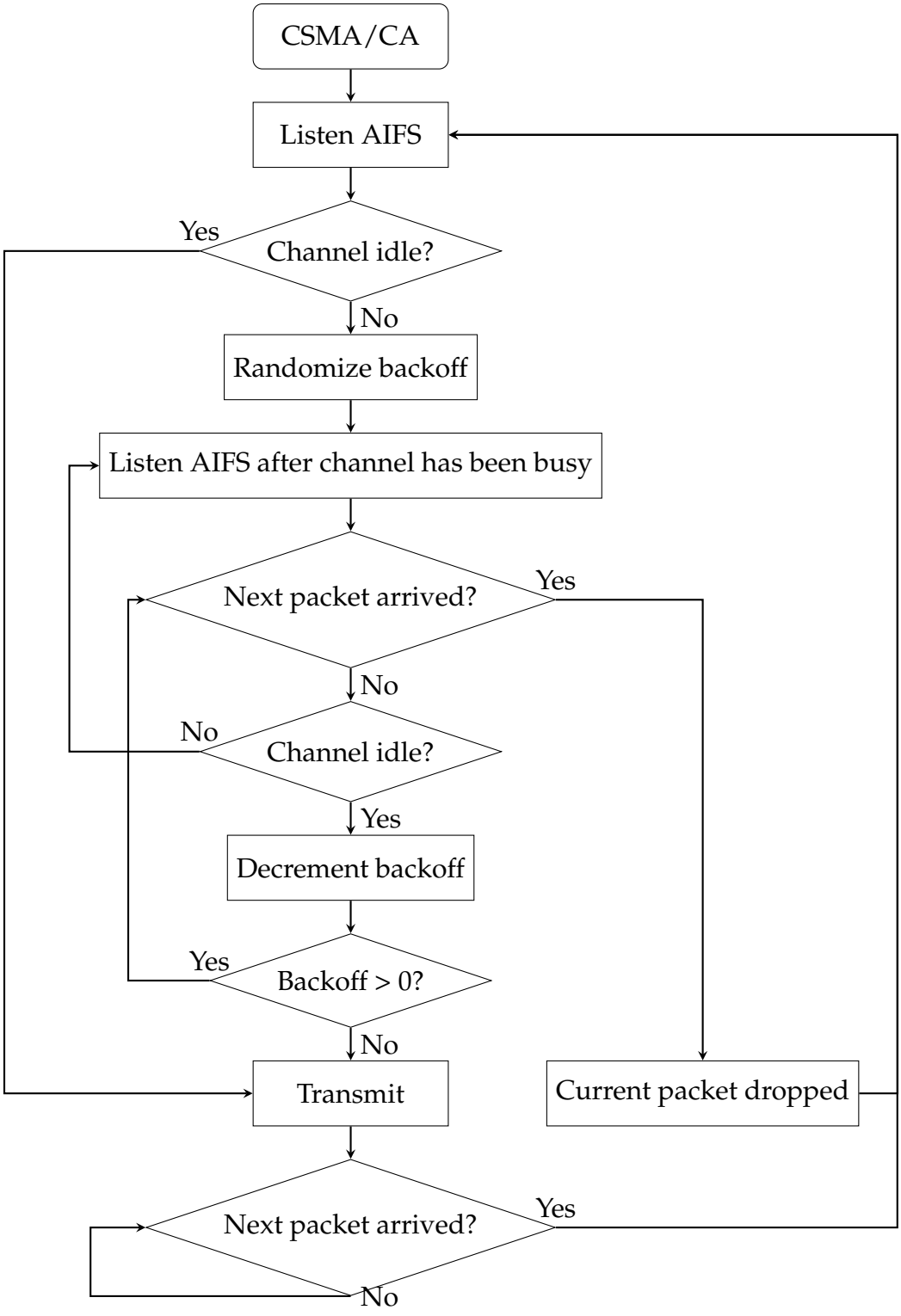

Figure 4.1: Broadcast CSMA/CA [Reprinted from [1]].

The 802.11 MAC protocol is a stop-wait-transmit protocol following the $RTS - CTS - Transmit - ACK$ handshaking scheme in the case of unicast scenario (RTS, CTS are optional). Packet loss in any part of the handshaking or no ACK results in retransmission of whole packet. For every increment in the number of attempts to transmit the packet, size of contention window is doubled from its initial value (CW_{min}) i.e., a binary exponential back-off is performed until CW reaches its maximum value (CW_{max}). Only a successful transmission or a packet drop resets the CW to its initial value.

In the case of broadcast scenario, the receiving nodes do not send any acknowledgments (ACK). As a result, the sender never knows whether the packet is successfully delivered or not. The sender at-most performs only a single back-off and the contention window will always be set to CW_{min}. The default values of the four priority queues in EDCA and their respective CW parameters are listed in the Table 4.1.

Priority	**Queue**	$\boldsymbol{CW_{min}}$	$\boldsymbol{CW_{max}}$	$\boldsymbol{AIFS_N}$
Lowest	1	$aCWmin$	$aCWmax$	9
	2	$aCWmin$	$aCWmax$	6
	3	$\frac{(aCWmin+1)}{2} - 1$	$aCWmin$	3
Highest	4	$\frac{(aCWmin+1)}{4} - 1$	$\frac{(aCWmin+1)}{2} - 1$	2

Table 4.1: Default parameter values of CW and $AIFS_N$ in 802.11p.

The minimum channel sensing period, T_{AIFS} is calculated according to:

$$T_{AIFS} = AIFS_N \times aSlotTime + aSIFSTime,$$

where $aSlotTime$ and $aSIFSTime$ (short interframe space, $SIFS$) are derived from

the OFDM PHY layer parameters.These are listed in Table 4.2.

Parameter	Value
$aCWmin$	15
$aCWmax$	1023
$aSlotTime$	13 μs
$aSIFSTime$	32 μs

Table 4.2: Parameter values for OFDM PHY

Table 4.3 gives the calculated values for different priority modes. T_{AIFS} values are calculated for broadcast mode with $CW = CW_{min}$. It can be seen that a minimum of 58 μs wait time (T_{AIFS}) is needed for an user to transmit in highest priority broadcast mode.

Priority	**Queue**	$\boldsymbol{CW_{min}}$	$\boldsymbol{CW_{max}}$	$\boldsymbol{T_{AIFS}(\mu s)}$
Lowest	1	15	1023	149
	2	15	1023	110
	3	7	15	71
Highest	4	3	7	58

Table 4.3: Calculated CW_{min}, CW_{max} for different priority modes in 802.11p

4.3 Limitations of CSMA/CA in VANETs

By observing the calculated values from Table 4.3, it can be concluded that a minimum channel access time of 58μs is needed for an user to transmit in broadcast mode with highest priority after the channel has become idle. EDCA methodology, when used in an ad-hoc network where all users have full connectivity is predictable. However, in a VANET scenario, where users are not fully connected

to other users, its no longer predictable due to the hidden terminal problem in CSMA.

CSMA/CA used in 802.11 networks faces further problems in case of real-time communications. Real-time communications generally imply that packets are to be delivered in a timely fashion with a certain error probability(reliability). Therefore *packet deadline* and *reliability* are the two important factors to be taken into consideration for real-time networks.

In a multi-user network with a channel access contention scheme in use, the total MAC-to-MAC delay in a packet transmission can be divided mainly into three categories namely:

- *Channel access delay*: time required for a packet received from MAC or above layer to be sent to the PHY layer for transmission in the presence of a MAC contention scheme.

- *Transmission delay*: total time required for a packet sent from a transmitter to reach a receiver in a wireless medium.

- *Decoding delay*: time required for a receiver to decode the packet. Depends on the decoding algorithm and the hardware performance.

It can be inferred that under the usage of a single contention scheme; MAC channel access delay has the major performance impact of the three in a multi-user network and can be controlled by proper design of contention scheme whereas the the two others almost remain constant [1].

Therefore, MAC channel access delay can be considered as a factor for packet deadline in real-time networks. As a result, a contention scheme providing an upper bound on channel access time (i.e., deterministic contention scheme) can be

considered necessary for real-time networks. Since major applications of VANET's are considered real-time in nature, the same logic holds good in case of VANET's.

CSMA as MAC is not able to support real-time deadlines in VANET's with increased network load as the access delay is not upper bounded (finite) resulting in packet drops. However, it is easily deployable due to its non-deterministic nature. A centralized scheme such as TDMA or FDMA can be useful in real-time scenarios but however, VANETs are decentralized (ad-hoc) in nature with individual users being highly mobile.

Therefore, a MAC scheme for VANET's should be able to solve the following three problems:

- be decentralized (adhoc) in nature.
- provide an upper bound on MAC channel access delay.
- be able to solve the hidden terminal problem with the ability to dynamically adjust with the increase/decrease in number of users in network.

The main aim of this thesis is to propose the use of slotted ALOHA with interference cancellation as an alternative to CSMA/CA and it is explained in detail in the subsequent sections.

4.4 ALOHA Protocols

The concept of random access for multiple users via ALOHA technique dates back to 1970's. In a pure ALOHA scheme, each user transmits its data packet as soon as it is formed. As a result, if 2 or more users transmit at same time, their packets collide resulting in loss of information and the packet data must be retransmitted. ALOHA scheme works well when the users in a network are relatively low. Assuming that a channel load of G is given to a system, its throughput

(T) under pure ALOHA is given as

$$T = Ge^{-2G}$$

A maximum throughput of 18% is achieved at channel load of 0.5. Since in pure ALOHA, users can start transmissions at any time resulting in performance inefficiency, slotted ALOHA was proposed where time is assumed to be slotted in time-slots of fixed duration with users starting their packet transmissions only at the beginning of time-slot. This results in an increase in an throughput as there is no overlap in between the slot durations. The resulting throughput is given by

$$T = Ge^{-G}$$

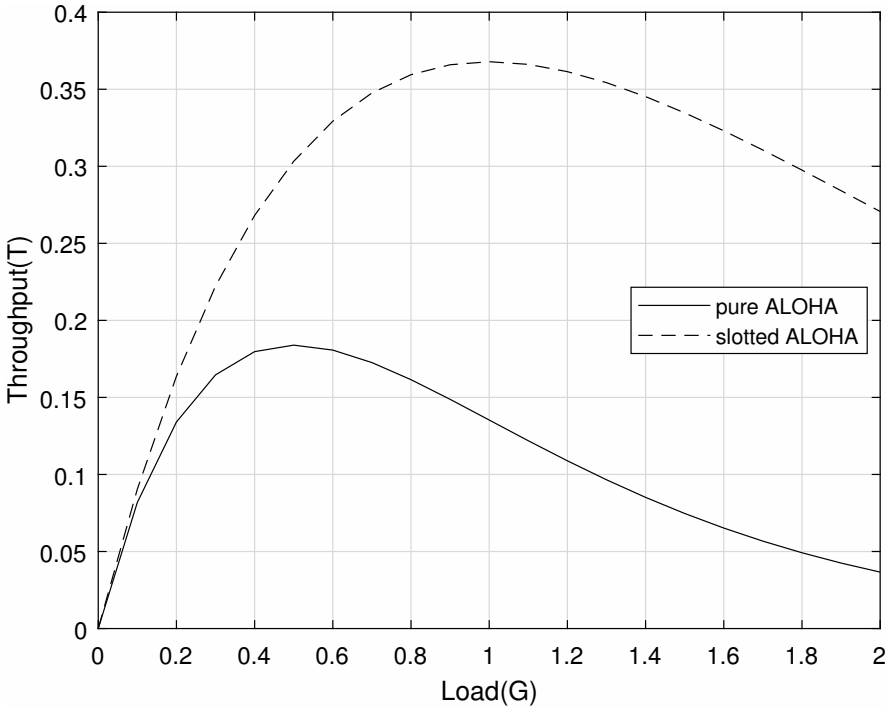

Figure 4.2: Throughput of pure and slotted ALOHA

under a channel load of $G = 1$ a maximum throughput of 37% is achieved. Figure 4.2 shows a comparison between pure and slotted ALOHA with respect to throughput and the channel load offered.

Slotted ALOHA still requires synchronization between all users in network, causing significant overhead. Collisions still occur when multiple users attempt to transmit in same slot. CSMA/CA with handshaking and random back-off can be used to further improve the throughput performance.

5. INTERFERENCE CANCELLATION BASED SLOTTED ALOHA

5.1 Introduction

Recently, MAC approaches based on multiple packet transmission via slotted ALOHA mechanism and interference cancellation in an iterative manner have been shown to improve the throughput performance substantially for some ideal channel models. Maximum throughput of 70-80% has been achieved in these proposed results.

Contention resolution diversity slotted ALOHA (CRDSA) was the first of such approaches and was proposed for satellite access packet networks for use with European digital video broadcasting (DVB) standard [11, 10]. In CRDSA, two copies of each packet are sent randomly in two different time slots within a MAC frame and packets are decoded using successive interference cancellation (SIC). Each packet possess information regarding the slot where the other replica was sent. Due to SIC, CRDSA improves the throughput performance to 55%.

Further improvements to CRDSA were proposed by generalizing it and allowing users to transmit more than 2 replicas where the actual number of packet copies to be sent is drawn from a degree distribution (probability mass function), which is optimized to achieve throughput performance for a specified load on the medium[13]. As the number of user transmitted replicas vary from user to user based on degree distribution, this scheme is referred to as irregular repetition slotted ALOHA (IRSA). As long as the number of users are less than the number of available of slots, IRSA with SIC improves the throughput performance depending on the degree distribution chosen.

5.2 IRSA Implementation

A bipartite graph based example for IRSA is shown in Figure 5.1. The implementation procedure is explained in detail in steps below:

- All users in a network decide on fixed packet size and format.
- Each user transmits a random number of replicas of the same packet in a single MAC frame divided into a number of time slots. The random number is drawn from a degree distribution ($\lambda(x)$) optimized for the network parameters and is known to all users in the network.
- Each packet transmitted contains information regarding the pointers to its copies i.e., the time slots in which the replicas are transmitted.
- Each user buffers the received signal whenever it is not transmitting. The buffered signal received by an user at slot i can be written as

$$y_i = \sum_{j \in U_i} h_{ij} x_j + w$$

  where x_j is a packet of the jth user, h_{ij} is its corresponding channel coefficient and w is the channel noise (AWGN). U_i is the set of all users that are able to transmit in the ith slot of a receiving user.
- A slot in which only one user has transmitted is called a singleton slot i.e., it contains only one packet. Since singleton slots do not contain any interference, each user decodes all the singleton slots in the MAC frame it has buffered.
- Channel coefficients corresponding to the copies of a successfully decoded packet are then estimated and its replicas at other slots are reconstructed.

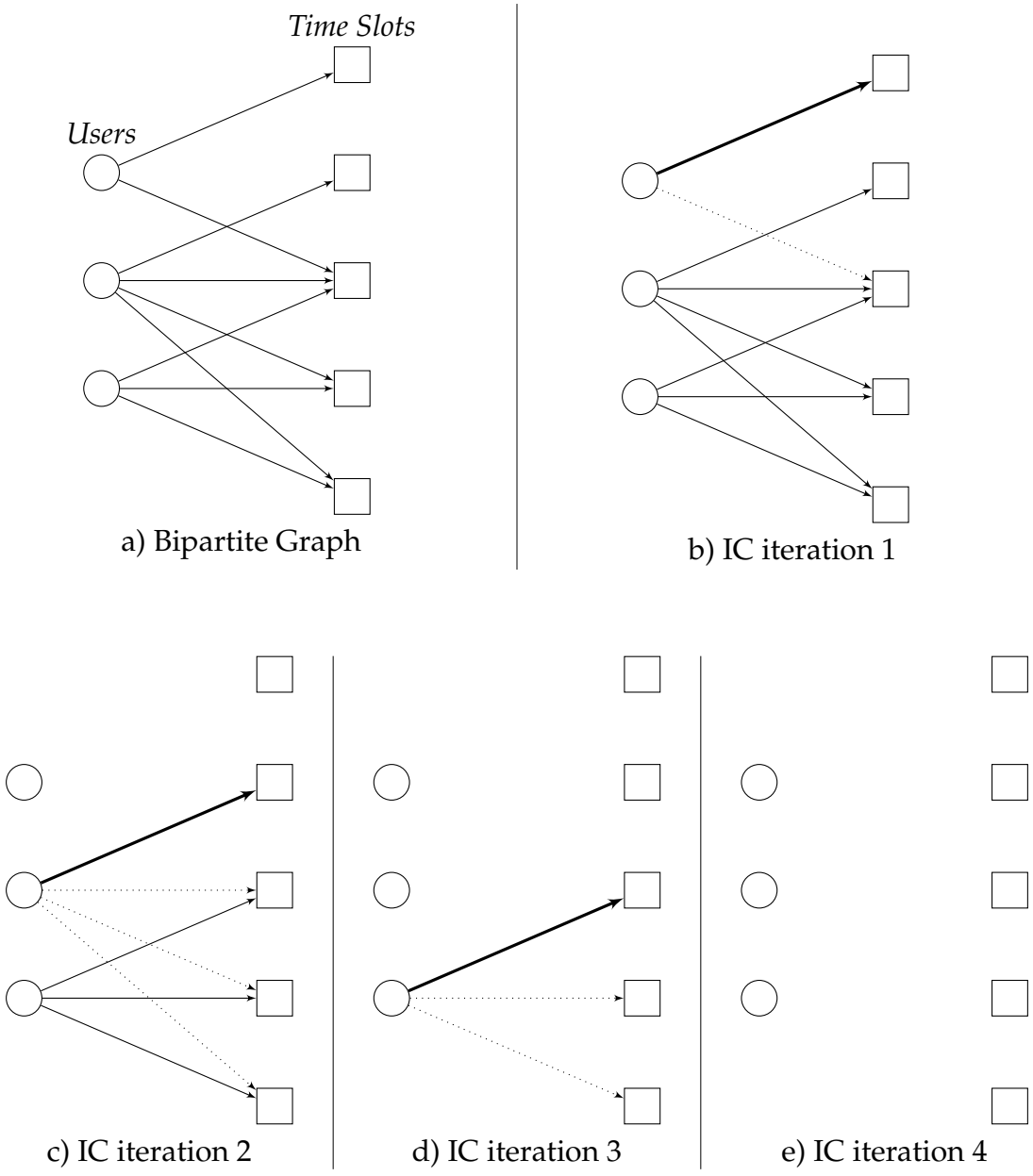

Figure 5.1: Bipartite Graph representation of the successive IC process

[Above figure shows the iterative decoding process used in IRSA.
Users are denoted by circles and time slots by squares.
Each edge denotes a transmission by an user in a time slot.
Degree distribution used in this example is : $\lambda(x) = \frac{1}{3}(x^2) + \frac{1}{3}(x^3) + \frac{1}{3}(x^4)$.
At each iteration singleton slots (denoted by thick arrow) are decoded and the copies of corresponding packet (dashed arrows) are cancelled out.]

The interference cancellation (IC) algorithm then works by canceling all the replicas that are reconstructed. If a kth user is being decoded and has its replica at ith slot, then the signal at ith slot after IC is,

$$\tilde{y}_i = \sum_{j \in U_i} h_{ij} x_j + w - \tilde{h}_{ik} x_k$$

or

$$\tilde{y}_i = \sum_{j \in (U_i - k)} h_{ij} x_j + w + h_{ik} x_k - \tilde{h}_{ik} x_k$$

where $\tilde{h}_{ik}$ is the estimated channel coefficient.

- Decoding proceeds further after subtracting the interference caused by the identified copies in a successive fashion until no more singleton slots are found.

The following *assumptions* are being made for executing IRSA.

- all users present in a network are both frame and slot synchronized. (can be achieved by GPS providing absolute time reference or by other means).
- the receiver is able to estimate the channel state information of packet replicas of successfully decoded packets with good accuracy.
- each user in network transmits only one packet in a MAC frame (copies of same packet are allowed but not different packets).

5.3 Performance evaluation in IRSA

Assuming that there are m users in a network with total of n time slots in a single MAC frame, the channel load in the network is given by

$$G = m/n$$

A packet transmission attempt that does not get decoded by an user is defined as packet loss. In other words , if an user k is not able to decode w users out of m users, the MAC packet loss ratio is given by

$$PLR_{MAC} = w/m,$$

Here user k is considered as a receiver. The throughput T of the MAC scheme is then given by the average number of successful packet transmissions per slot as:

$$T(G) = G(1 - PLR_{MAC}(G))$$

and

$$PLR_{MAC}(G) = 1 - \frac{T(G)}{G}.$$

IRSA scheme works best when the number of users in a network (m) are less than the number of available slots (n). Since IRSA scheme operation works on the basis of graph codes applied on packet level, the scheme works best as the total number of slots, $n \to \infty$.

5.4 Application of IRSA to VANETs

As discussed in the above sections, it has been shown that a MAC scheme for vehicular networks should be decentralized, deterministic and mitigate the hidden node problem. In case of IRSA, since slotted ALOHA is a random access protocol only with the backdrop of network synchronization, it can be considered as applicable to decentralized ad-hoc networks.

As long as the number of users are less than the number of slots, or for an asymptotically large number of slots, IRSA is considered to perform reasonably

well with each user transmitting in at least one slot per a MAC frame. By setting the length of the MAC frame and the packet size within reasonable limits, it can be shown that the MAC channel access time in IRSA is upper bounded with the bound being the length of MAC frame if all the users are being successfully decoded.

The problem of hidden terminals also does not exist in IRSA, as collisions are used for decoding via SIC. CSMA on other hand, requires sensing of channel and can still be affected by hidden terminal problem in a real vehicular network [8].

Even though IRSA presents promising results, it cannot perform optimally in channel overload problems, resulting from massive overload of devices compared to available slots, in the case of ad-hoc networks where the number of users in network is not known a priori, limiting its application in such scenarios.

A centralized controller/access point (AP) providing an estimate of number of users in a network and the optimized degree distribution can be useful in such a case. An example of such a frame structure is shown in Table 5.1 for the AP case.

The base station uses a beacon to obtain coarse synchronization and channel gains (h_i). During this beacon period each user transmits a signature sequence scaled by $1/h_i$. Then, the base station estimates the number of users in network, from which it calculates the number of slots M and degree distribution and broadcasts it. Each user then picks these values and transmit their packets in time slots.

			<——————Frame Length M——————->					
Beacon	Estimate No. of users	*GI*	Slot 1	*GI*	.....	*GI*	Slot M	*GI*

GI - Guard Interval

Table 5.1: Frame format for IRSA scheme with a centralized access point

Finally, the SIC algorithm increases the number of computations at receiver and hence the hardware complexity further limiting its applications. A trade-off between application requirements and the receiver complexity is needed.

5.5 Our Implementation of IRSA

As the IRSA scheme works in a similar way of decoding bipartite graphs using SIC, a similar simulator was developed in MATLAB where, by specifying the number of time slots n and degree distribution $\lambda(x)$, each user in a multi-user network generates packets based on the distribution and transmits them in randomly selected time slots using 802.11p PHY through a fading channel, both of which are simulated as described in Chapters 2 & 3.

At the receiver of each user, packets are stored for the complete MAC frame and the singleton slots are decoded in an iterative fashion until all users are decoded or until no more singleton slots are left behind. The following cases are be considered as factors for packet loss while decoding:

- packet corruption during transmission through wireless channel.
- stopping sets in bipartite graph where a set of users choose exactly same slots for transmission, rendering SIC useless.

Finally, average packet loss ratio and throughput are calculated using the expressions mentioned above.

6. SIMULATION RESULTS

To evaluate the performance of IRSA for vehicular networks, a joint PHY-MAC simulator was implemented using MATLAB. The complete code is made available in *Github*.

An OFDM scheme based physical layer transceiver is implemented as mentioned in Chapter 2. Empirical wireless channel models for vehicular networks described in Chapter 3 based on Tap-Delay line model [6, 17] and Cheng's model [7] were used to evaluate the performance and reliability of physical layer under realistic vehicular conditions. The simulation parameters are listed in Table 6.1.

Parameter	**Variable**	**Value**
PHY parameters for QPSK rate - $1/2$ ***- OFDM***		
Data Rate	r_{data}	6 Mbps
PHY preamble duration	t_{prm}	$40\mu s$
Packet size assumed	d_{pack}	400 bytes
CSMA Parameters (for packet priority-highest)		
CSMA slot duration	t_{csma}	$13\mu s$
AIFS time	t_{aifs}	$58\mu s$
Simulation parameters used in IRSA		
Frame duration	t_{frame}	$100ms$
Guard interval assumed	t_{guard}	$5\mu s$
Packet length for 400 byte packet	t_{pack}	$576\mu s$
Slot duration for 400 byte packet	$t_{slot} = t_{guard} + t_{pack}$	$581\mu s$
Number of slots in a frame	$n = \lfloor t_{frame}/t_{slot} \rfloor$	172
Degree distribution used for IRSA	$0.86x^3 + 0.14x^8$	

Table 6.1: Simulation parameters

6.1 PER Analysis

The packet error rate plots for AWGN and vehicular channels mentioned in Acosta-Marum & Ingram Model [6] are plotted in Figure 6.1 as a function of E_b/N_o for a packet size of 400 bytes and 6 Mbps data rate. It can be observed that the Vehicle to Vehicle (V2V) channels have a relatively higher packet error rate when compared to Vehicle to Infrastructure (V2I/RTV) channels which can be attributed to their relatively higher Doppler shifts.

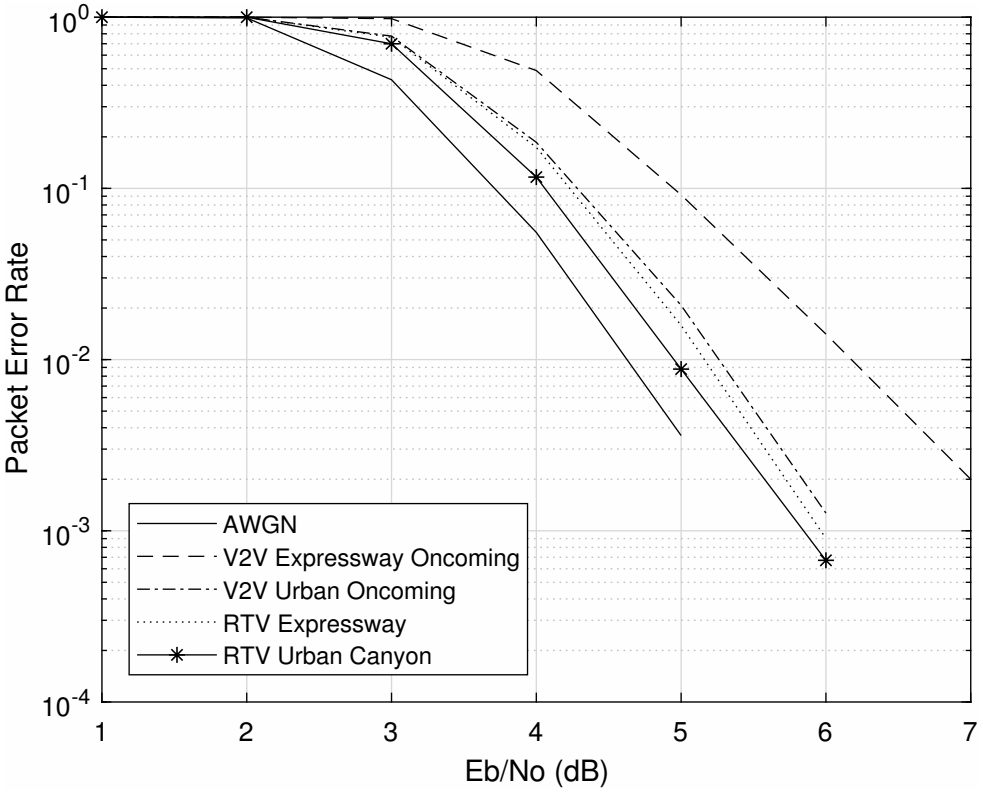

Figure 6.1: PER results for packet size of 400 bytes for QPSK with rate 1/2

6.2 Path Loss Analysis

Figure 6.2 shows a plot for the received signal strength with varying distance for a transmitted power of 20dBm. Large scale fading model for dataset 1 mentioned in Cheng's model [7] with dual slope path loss and shadowing is used for this simulation. Figure 6.3 shows plot for signal to noise ratio measurement with varying distance. The noise power is fixed at -99dBm for this simulation. A reception range varying from 200-500 meters can be achieved for this transmitted power.

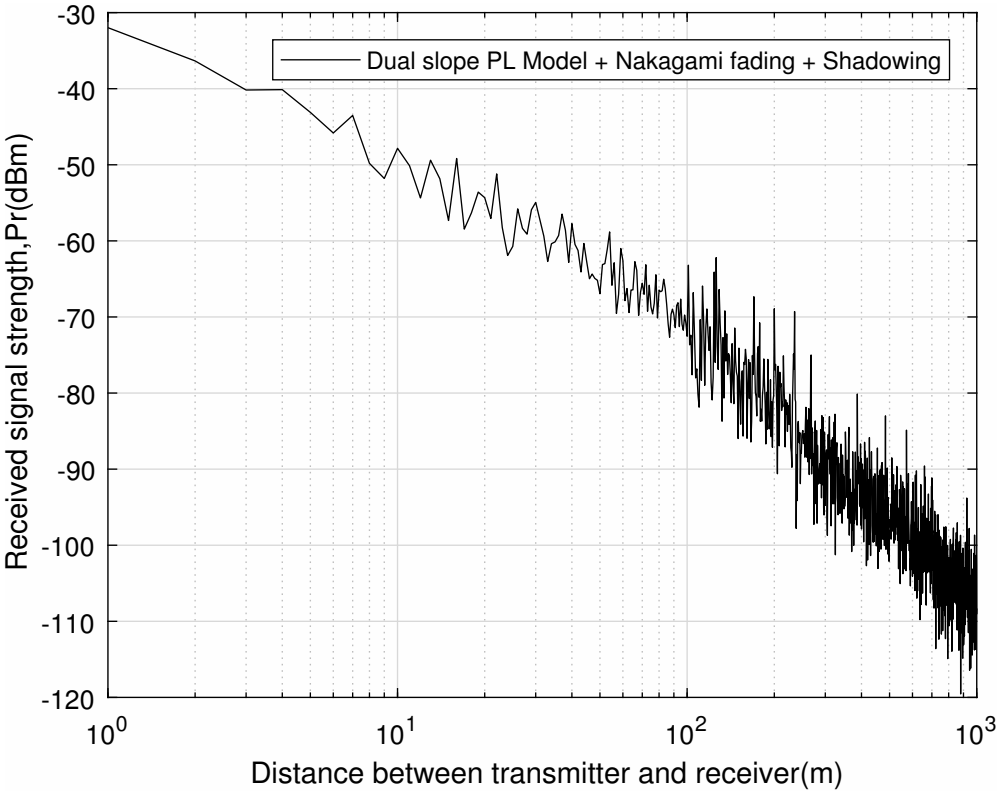

Figure 6.2: Recieved signal strength (dBm) for a transmitted power of 20dBm

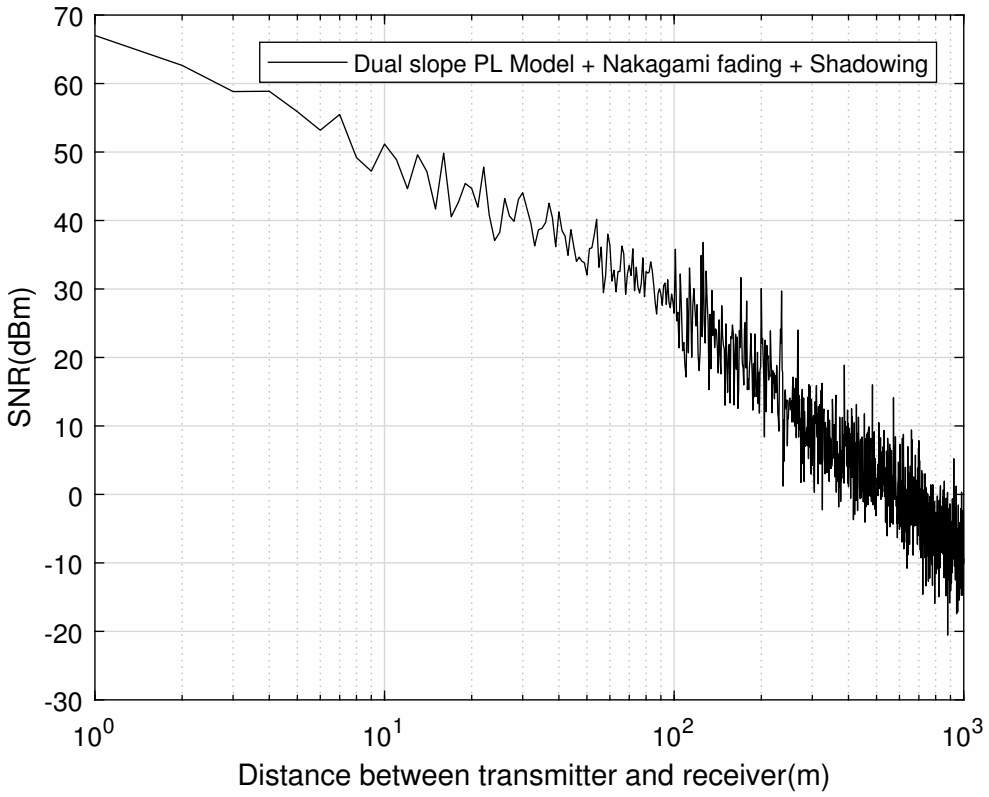

Figure 6.3: Signal to Noise Ratio (dBm) for a transmitted power of 20dBm and noise power of -99dBm

6.3 IRSA Performance Evaluation

To evaluate the performance of IRSA for VANET's with 802.11p PHY layer, *packet loss ratio* & *throughput* as functions of channel load are plotted in following sections. The parameters used for the simulation are listed in the Table 6.1.

6.3.1 Packet Erasure Channel

The packet loss ratio is first evaluated for different degree distributions of IRSA in an idealized packet erasure channel (PEC) with zero erasure probability ($\epsilon = 0$) to ensure the correct working of SIC algorithm and for verification with the existing results provided in [11, 8]. The results for packet loss ratio and throughput are plotted in Figures 6.4 and 6.5.

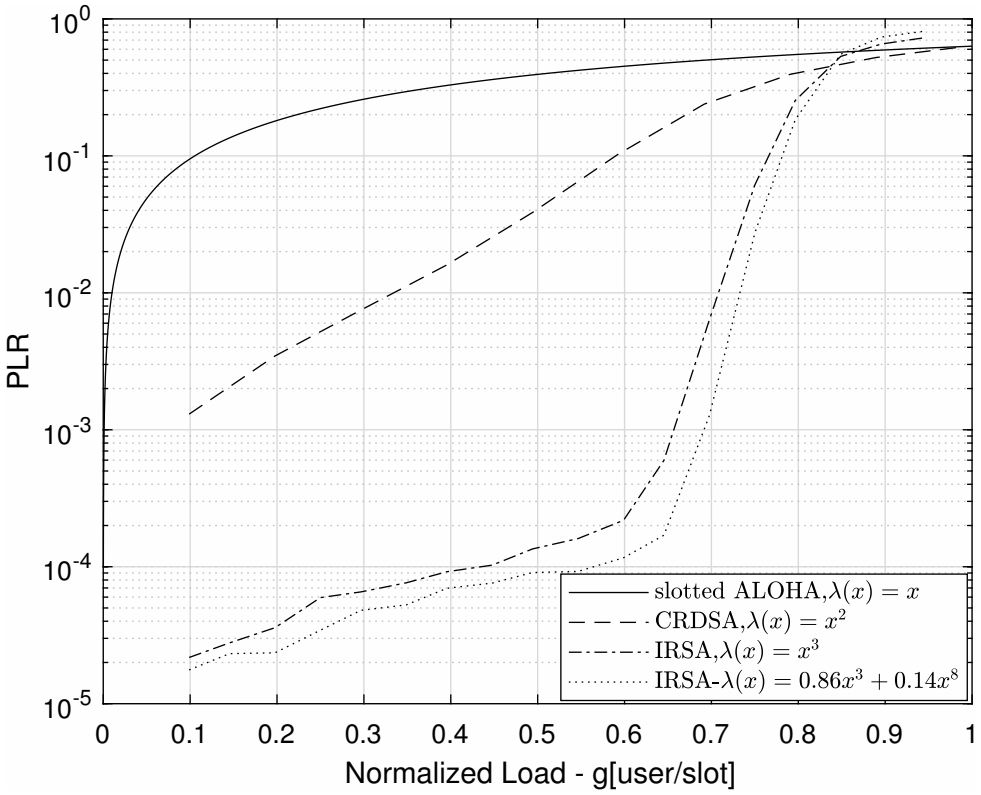

Figure 6.4: PLR results in packet erasure channel with $\epsilon = 0$

It can be observed from Figure 6.4 that an error floor exists in higher order degree distributions which is mainly due to stopping sets, where a set users cannot be resolved due to selection of same slots for transmission.

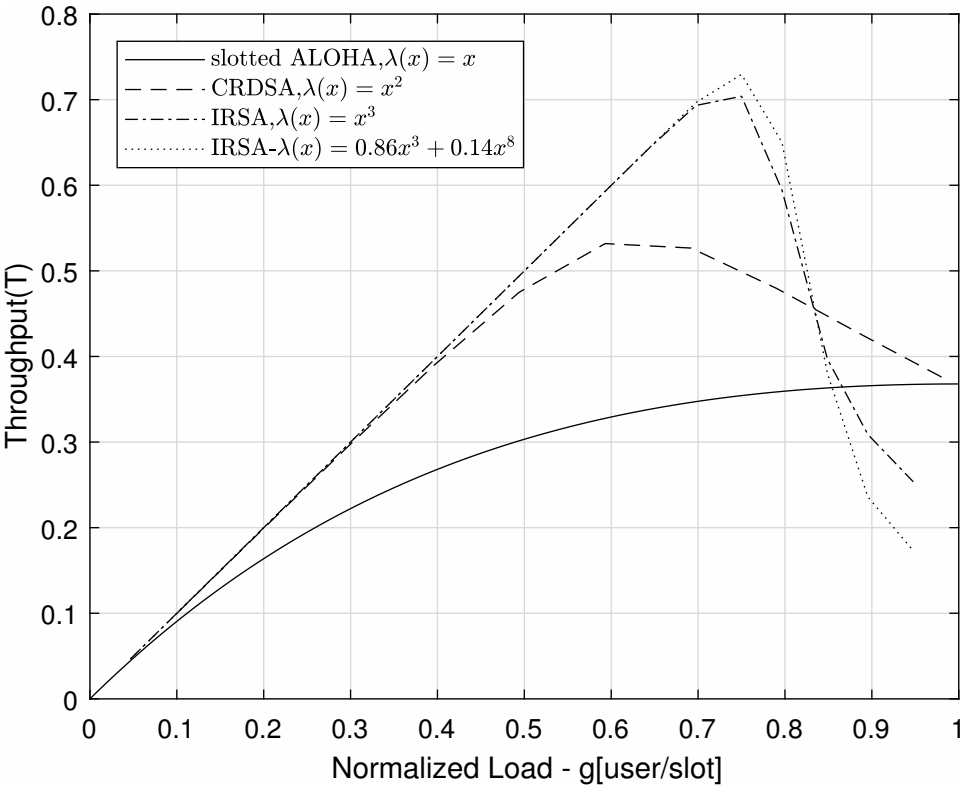

Figure 6.5: Throughput results in packet erasure channel with $\epsilon = 0$

6.3.2 Vehicular Channels

Finally, the packet error rate and throughput performance of IRSA with degree distribution of $\lambda(x) = 0.86x^3 + 0.14x^8$ in AWGN, V2V and V2I channels [6] with 802.11p PHY are presented in Figures 6.6 and 6.7.

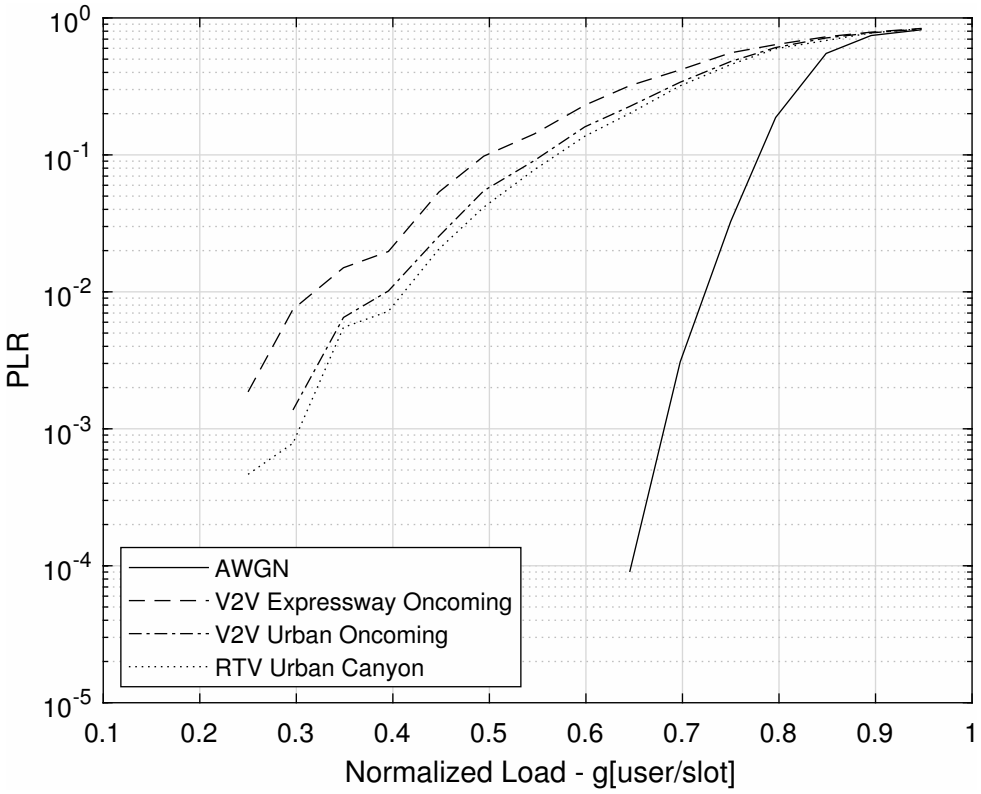

Figure 6.6: PLR results for packet size of 400 bytes for QPSK with rate $1/2$

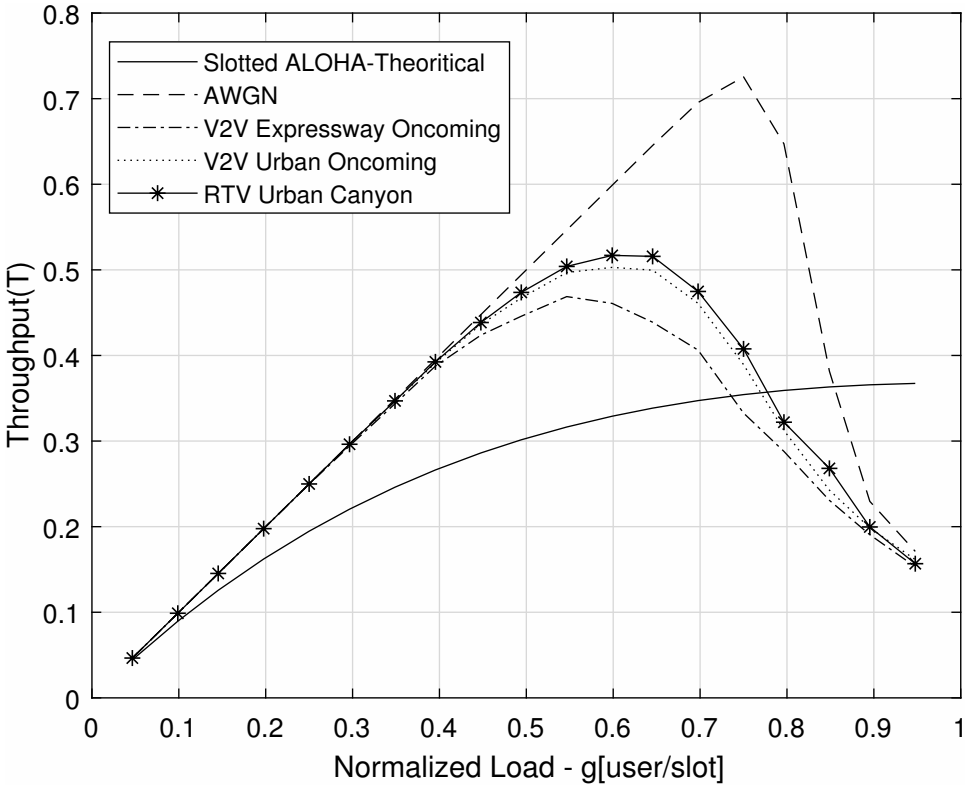

Figure 6.7: Throughput results for packet size of 400 bytes for QPSK with rate 1/2

It can inferred from Figure 6.7 that IRSA scheme results in a substantial improvement in throughput performance when compared to pure slotted ALOHA. Throughput close to 70% in AWGN channels and 50% in vehicular channels is achieved.

6.3.3 MAC Channel Access Delay

Figure 6.8 shows a CDF plot for the minimum channel access time required for the MAC layer algorithm in use (IRSA in this case) to send its packet in a multi-user scenario. This was calculated for the 100*ms* MAC frame duration for the IRSA scheme. It can be observed that all of the users in network obtain channel access during this duration. As observed in Figure 6.7, as long as the throughput remains equal to normalized channel load, all users transmit successfully (~40-50% of channel load in vehicular networks).

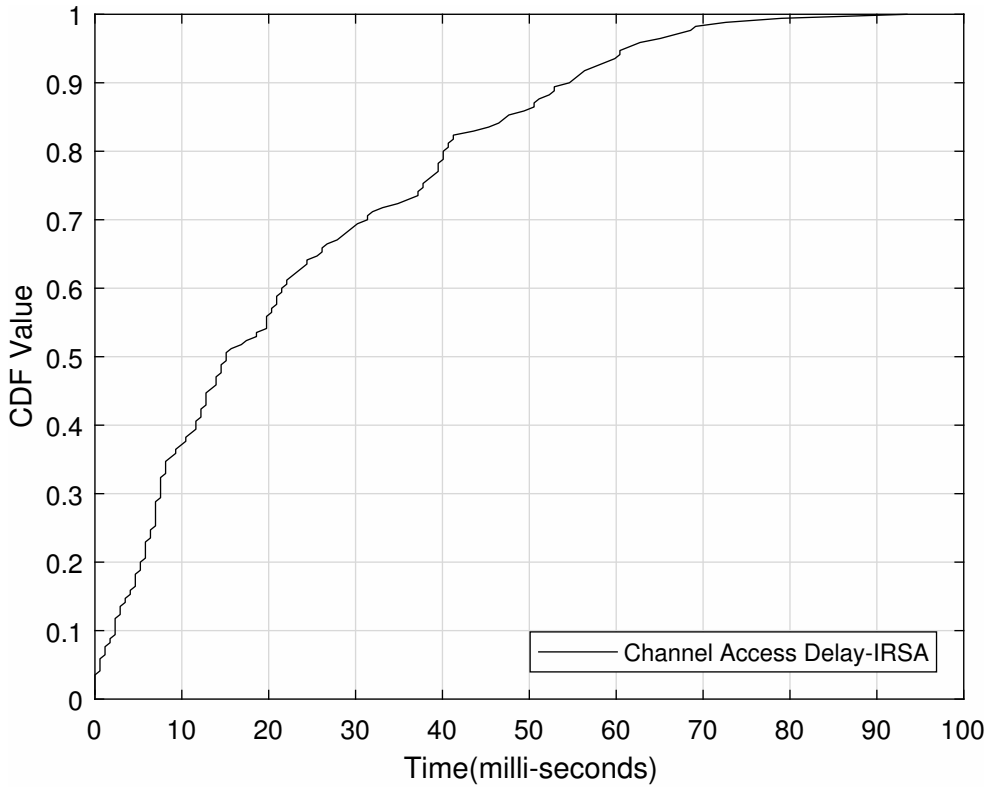

Figure 6.8: CDF of channel access delay for packet size of 400 bytes for QPSK with rate 1/2

7. CONCLUSION & FUTURE WORK

7.1 Conclusion

The work in this thesis focused on developing the following simulation models following in MATLAB.

- Implementing a baseband IEEE 802.11p transceiver.
- Implementation of successive interference cancellation based slotted ALOHA mechanism (IRSA) for improving the latency and throughput performance.
- Performance analysis of IRSA MAC scheme in the presence of realistic models for vehicular communication channels.

We have developed a software platform for evaluating PHY and MAC layer algorithm with realistic channel models and other parameters specified by the IEEE 802.11p. Using this software platform, we evaluated the performance of IRSA with SIC as an alternative MAC protocol for vehicular communications. Simulation results obtained in this thesis show that IRSA with SIC can provide substantially higher throughput than slotted ALOHA or CSMA without interference cancellation and should be considered as a viable alternative to CSMA/CA for vehicular communications.

7.2 Future Work

The IRSA analysis presented in this thesis uses the degree distribution optimized for a packet erasure channel [8]. Further optimization is needed for the case of realistic fading channels. Also, total transmission delay for a successful packet transmission for the IRSA scheme needs to calculated accurately. In partic-

ular channel access delay and decoding delay need to be optimized for real-time vehicular communications.

Channel estimation and equalization schemes also need to be optimized for 802.11p. LS/MMSE estimation schemes available in the literature using training sequences in packet preamble have been proposed to be used with CSMA/CA channel access scheme and without considering SIC. Further modifications to the preamble structure and estimation schemes are needed for the IRSA scheme.

Another very important direction of future work is in integrating the results from the software platform developed here along with control algorithms designed for intelligent transportation systems. In particular, delay profiles for traffic can be obtained using the simulation test bed developed here and the result of control algorithms can be studied using these delay profiles.

REFERENCES

[1] K. Bilstrup, E. Uhlemann, E. Ström, and U. Bilstrup, "On the ability of the 802.11 p MAC method and STDMA to support real-time vehicle-to-vehicle communication," *EURASIP Journal on Wireless Communications and Networking*, vol. 2009, no. 1, p. 902414, 2009.

[2] "IEEE Standard for Information technology–Telecommunications and information exchange between systems Local and metropolitan area networks–Specific requirements - Part 11: Wireless LAN Medium Access Control (MAC) and Physical Layer (PHY) Specifications," *IEEE Std 802.11-2016 (Revision of IEEE Std 802.11-2012)*, pp. 1–3534, Dec 2016.

[3] "IEEE Standard for Information technology– Local and metropolitan area networks– Specific requirements– Part 11: Wireless LAN Medium Access Control (MAC) and Physical Layer (PHY) Specifications Amendment 6: Wireless Access in Vehicular Environments," *IEEE Std 802.11p-2010 (Amendment to IEEE Std 802.11-2007 as amended by IEEE Std 802.11k-2008, IEEE Std 802.11r-2008, IEEE Std 802.11y-2008, IEEE Std 802.11n-2009, and IEEE Std 802.11w-2009)*, pp. 1–51, July 2010.

[4] A. M. Abdelgader and W. Lenan, "The Physical Layer of the IEEE 802.11 p WAVE Communication Standard: The Specifications and Challenges," in *Proceedings of the World Congress on Engineering and Computer Science*, vol. 2, 2014.

[5] I. Ivan, P. Besnier, X. Bunlon, L. Le Danvic, M. Crussière, and M. Drissi, "Influence of propagation channel modeling on V2X physical layer perfor-

mance," in *Antennas and Propagation (EuCAP), 2010 Proceedings of the Fourth European Conference on*, pp. 1–5, IEEE, 2010.

[6] M. A. Ingram, "Six time-and frequency-selective empirical channel models for vehicular wireless LANs," *IEEE Vehicular Technology Magazine*, vol. 2, no. 4, pp. 4–11, 2007.

[7] L. Cheng, B. E. Henty, D. D. Stancil, F. Bai, and P. Mudalige, "Mobile vehicle-to-vehicle narrow-band channel measurement and characterization of the 5.9 GHz dedicated short range communication (DSRC) frequency band," *IEEE Journal on Selected Areas in Communications*, vol. 25, no. 8, 2007.

[8] M. Ivanov, F. Brannstrom, A. G. i Amat, and P. Popovski, "Broadcast Coded Slotted ALOHA: a finite frame length analysis," *IEEE Transactions on Communications*, 2016.

[9] H. A. Cozzetti, R. M. Scopigno, L. Casone, and G. Barba, "Comparative analysis of IEEE 802.11 p and MS-Aloha in VANET scenarios," in *Services Computing Conference, 2009. APSCC 2009. IEEE Asia-Pacific*, pp. 64–69, IEEE, 2009.

[10] G. Choudhury and S. Rappaport, "Diversity ALOHA–A random access scheme for satellite communications," *IEEE Transactions on Communications*, vol. 31, no. 3, pp. 450–457, 1983.

[11] E. Casini, R. De Gaudenzi, and O. D. R. Herrero, "Contention resolution diversity slotted ALOHA (CRDSA): An enhanced random access schemefor satellite access packet networks," *IEEE Transactions on Wireless Communications*, vol. 6, no. 4, 2007.

[12] K. R. Narayanan and H. D. Pfister, "Iterative collision resolution for slotted ALOHA: An optimal uncoordinated transmission policy," in *Turbo Codes*

and Iterative Information Processing (ISTC), 2012 7th International Symposium on, pp. 136–139, IEEE, 2012.

[13] G. Liva, "Graph-based analysis and optimization of contention resolution diversity slotted ALOHA," *IEEE Transactions on Communications*, vol. 59, no. 2, pp. 477–487, 2011.

[14] C. F. Mecklenbrauker, A. F. Molisch, J. Karedal, F. Tufvesson, A. Paier, L. Bernadó, T. Zemen, O. Klemp, and N. Czink, "Vehicular channel characterization and its implications for wireless system design and performance," *Proceedings of the IEEE*, vol. 99, no. 7, pp. 1189–1212, 2011.

[15] H. Abdulhamid, E. Abdel-Raheem, and K. E. Tepe, "Channel tracking techniques for OFDM systems in wireless access vehicular environments," in *Signal Processing and Its Applications, 2007. ISSPA 2007. 9th International Symposium on*, pp. 1–4, IEEE, 2007.

[16] S. Colieri, M. Ergen, A. Puri, and A. Bahai, "A study of channel estimation in OFDM systems," in *Vehicular Technology Conference, 2002. Proceedings. VTC 2002-Fall. 2002 IEEE 56th*, vol. 2, pp. 894–898, IEEE, 2002.

[17] C.-D. Iskander and H.-T. Multisystems, "A MATLAB-based object-oriented approach to multipath fading channel simulation," *Hi-Tek Multisystems*, vol. 21, 2008.